THE JOURNAL OF PHYSICAL CHEMISTRY C

Article

pubs.acs.org/JPCC

Controlling the Performance of a Three-Terminal Molecular Transistor: Conformational versus Conventional Gating

Saikat Mukhopadhyay and Ravindra Pandey*

Department of Physics, Michigan Technological University, Houghton, Michigan 49931, United States

Shashi P. Karna*

U.S. Army Research Laboratory, Weapons and Materials Research Directorate, ATTN: RDRL-WM, Aberdeen Proving Ground, Maryland 21005-5069, United States

Supporting Information

ABSTRACT: The effect of conformational changes in the gate arm of a three-terminal device is investigated. In the ground state, the gate (triphenyl) arm is nonplanar, where the middle phenyl ring is approximately 30° out-of-plane relative to other two rings. At this geometry, the calculated tunnel current (I_d) as a function of external bias (V_{ds}) across the two D−A substituted arms exhibits a typical insulator-semiconductor behavior. Similar I_d−V_{ds} characteristics is calculated when planarity of the triphenyl arm is restored. However, a significant increase, by more than an order of magnitude, and a distinct variation in the current are predicted in its operational mode (V_{ds} > 1.5 V) when additional nonplanarity is induced in the triphenyl chain. Analysis of the results suggest that, unlike in "voltage" gating, neither the HOMO−LUMO gap nor the dipole moment of the system undergo significant changes due to pure conformational gating, as observed in this study. Instead, the observed conformational gating affects the current via localization/delocalization of the electronic wave function in the conduction channel. Furthermore, the tunneling current corresponding to conformational gating in two different directions appears to exhibit oscillatory nature with a phase factor of $\pi/2$ in the presence of the gate field. The current modulation is found to reach its maximum only under exclusive effect of voltage or conformational gating and diminishes when both of them are present.

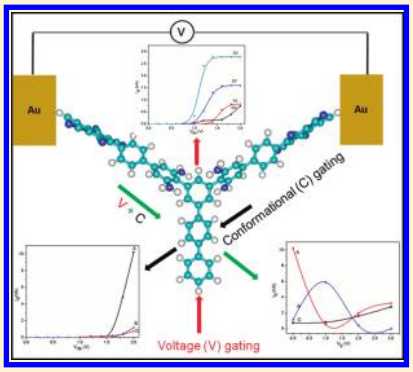

1. INTRODUCTION

Molecular-scale electronics has been a subject of intense experimental[1−7] and theoretical studies[8−18] in the past decade aiming to use organic, inorganic (nanostructured materials), and biological molecules as active elements of electronic devices. In the case of organic molecules, several pioneering experiments to measure current (I)−voltage (V) characteristics of single molecular structures in two-terminal (wire) configurations have been reported. In keeping with experiments, extensive theoretical investigations have been performed to explain observed experimental results as well as to develop detailed fundamental understanding of the underlying physics and chemistry. An ambitious but technically challenging goal in the molecular scale electronics is to realize three-terminal devices,[11,19−25] where the current through a molecular architecture under bias can be modulated by a second gate field, analogous to the current in inorganic field-effect transistors (FETs). Theoretical studies by He et al.[12] have shown that such an FET can be realized in a donor−acceptor (D-A) junction (J)-A-D architecture by applying a second field across a third arm of triphenyl ring connected to the junction. The switching effect is noted to result from the modulation of the wave function and energies of molecular orbitals (MOs) as well as the dipole moment of the molecule as a function of the applied gate field. Ghosh et al.[11] and Perrine et al.[16] have investigated the effects of a gate field in several simpler organic structures under bias. Experimental observation of electric-field gating in a single organic molecule has been reported in a number of recent articles.[4,5,22]

Electric-field gating of organic molecular current under bias is a natural extension of the recent microelectronics FETs; however, it is not as desirable as in microelectronics because of the technical challenges associated with the assembly of organic molecular systems in appropriate orientation and the requirements of applying a second external field, which potentially would induce additional changes to the electronic and geometric structure of the molecule. Also, it does not fully utilize the versatility of the structure-electronic property relationships of organic molecules. For example, organic molecular architectures offer the possibilities of chemical/structural gating in which the change in the structure due to molecular rotation, conformational change, or coupling of vibrational modes with electronic modes can modulate tunneling current across the molecule under biased condition.

Received: September 16, 2011
Revised: January 17, 2012
Published: January 24, 2012

In fact, chemical gating, in general, is a dominant phenomenon in a wide range of naturally occurring biological process, such as bacterial photosynthetic reaction centers,[26−28] protein reactions,[29,30] and KcsA potassium channel.[31] The chemical gating also plays a key role in the mechanism for the enzyme specificity.[32] Even though it is obvious that "conformational gating" is very common in nature, it has not received full attention for molecular electronics.

In a typical donor-bridge-acceptor architecture, the electron transfer (ET) is shown to depend critically on the conformational change (e.g., torsion angle) given to its molecular moieties.[33] Theoretical studies on organic molecular wires[11,34] also suggest strong current modulation due to conformational changes. A recent experiment by Venkataraman et al.[35] has also shown the dependence of electronic conductance on the molecular conformation.

In the present study, we show by first-principles quantum mechanical calculations that chemical gating due to change in conformation in the unbiased (third) branch of a three-armed organic structure, similar to the one used by He et al.,[12] can lead to an order of magnitude current switching across the conducting arms under biased condition. Application of second field to the conformational-gated high-conducting (ON) state of the molecule appears to switch OFF and again ON (with reduced magnitude of current) by a phase factor, $\phi = \pi/2$. In contrast, application of second field across the third arm of the molecular architecture under biased condition exhibits usual voltage gating effect accompanied by a decrease in threshold voltage (V_{ds}) with increasing gate bias. We compare the effects of chemical and voltage gating and show the dependence of voltage gating on the geometry (conformation) of the third branch in the three-terminal architecture.

2. COMPUTATIONAL DETAILS

As shown in Figure 1, the three-terminal molecular architecture considered in this study consists of two diode units, namely,

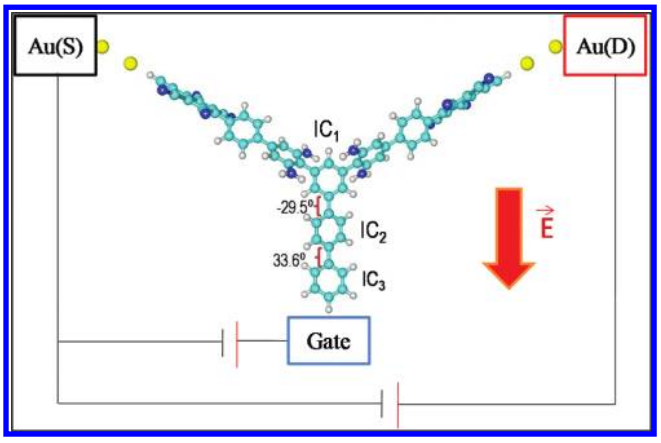

Figure 1. Schematic diagram of the setup of a unimolecular transistor-like device ABD-IC-DBA. C, N, H, and Au atoms are depicted by green, blue, white, and yellow spheres, respectively. A positive bias is applied at the source (S) and a gate field "E" is applied in the direction as shown.

ABD and DBA, in which the donor (D) and acceptor (A) moieties are derived from 1,3-diaminobenzene and 1,2,4,5-tetracyanobenzene, respectively. The π-conjugated phenyl ring was used as the bridge (IC_1) between the diode structures. The bridging phenyl ring is also covalently bonded to the π-conjugated triphenyl moieties (IC_2 and IC_3), referred to here as the "gate (G)" arm, by analogy to the microelectronic FETs. The model architecture is likely to translate the internal conducting states with respect to the pseudo-Fermi level, as described in a previous study[36] on a model biphenyl molecular transistor. In this study, the conformational changes of the system are considered by rotating IC_2 relative to IC_1 in the clockwise (i.e., outward rotation) and the anticlockwise (i.e., inward rotation) directions by 30°.

As noticed from Figure 1, the system is symmetric along the source (S)-drain (D) direction (with a zero dipole component), whereas it is asymmetric in the gate direction (with a large dipole component). Semi-infinite gold nanowires are used to design the source and drain electrodes. In general, S is used as a linker atom between the molecule and Au electrode. This is due to the fact that S has a greater affinity to covalently bind with Au atoms. However, the presence of S-linker atom creates undesired effects, such as the formation of frontier orbitals of the extended molecular system and Au−S hybridized states in the gap between the highest occupied and the lowest unoccupied MOs, which mask the true effects due to the molecular geometrical and electronic structures.[37,38] To avoid such effects, we used a H-terminated molecular architecture. In addition, H-terminated molecule between the Au leads also mimics the weak metal−molecule bonds in non-thiol-terminated self-assembled monolayers of organic molecules. The H−Au bond was set to 2.0 Å following the previously reported H-metal adsorption distance.[39] We are aware of the errors that might arise due to the simplicity in designing the electrodes and contacts. To validate our approach to model the contact and electrodes and justify the relevance of our theoretical approximations in real experiments, we have compared our results with the experimental study on ODT-based molecular transistor.[4] Interestingly, our calculated results were found to be in great agreement with that reported in the experiments. (Please see Figure S1 in the Supporting Information.) The positive gate field is defined with respect to the direction of the dipole moment of the molecule, as shown in Figure 1.

The electron transport calculations were carried out in two steps: (A) In the first step, electronic-structure calculations were performed on the extended molecular complex consisting of Au-molecule-Au, instead of "an isolated molecule", in the framework of the density functional theory (DFT) with B3LYP functional form[40,41] and the LanL2DZ basis set as implemented in Gaussian 03.[42] The B3LYP functional form and LANL2Z basis set were also used successfully in our previous studies on electron transport in molecular systems.[43,44] It is worth noting that the calculated results obtained at the B3LYP-DFT level of theory is not likely to match the accuracy of the results obtained using GW approximation, although recent investigations on Au-benzene-Au have treated only the molecule with GW approximation while considering the electronic structure of the contact gold in the DFT level of theory.[45] Because our focus is on predicting qualitative features of electronic transport of the extended molecular complex, we believe that treating both contact and the molecule at the DFT level of theory[44,46] is a viable alternative. The extended molecular complex is the core-scattering region of the molecular transport system, composed of the molecule and atomic-scale gold contacts in the form of atomic wire coupled to the source and drain electrodes. (B) The I_d-V_{ds} characteristics of the molecular complex were calculated using Green's function-based Landauer−Büttiker formalism[47−49] in the framework of the DFT. In this

dx.doi.org/10.1021/jp208983d | J. Phys. Chem. C 2012, 116, 4840−4847

approach, the tunneling current (I_d) as a function of the applied bias (V_{ds}) in such a device can be expressed as

$$I_d = \frac{2e}{h}\int_{-\infty}^{\infty} dE\ T(E, E_g)[f(E-\mu_1) - f(E-\mu_2)] \quad (1)$$

where μ_1 and μ_2 are the electrochemical potentials in the source and drain electrodes under an external bias V_{ds} and $f(E)$ is the Fermi−Dirac distribution function. For instance, a positive bias lowers the electrochemical potential at the drain by eV which may be expressed as

$$\mu_1 - \mu_2 = eV \quad (2)$$

and gives rise to different Fermi−Dirac distribution functions at the source and the drain

$$f(E-\mu_1) = \frac{1}{e^{[(E-\mu_1)/(K_BT)]+1}}$$
$$f(E-\mu_2) = \frac{1}{e^{[(E-\mu_2)/(K_BT)]+1}} \quad (3)$$

which is the driving force for generating the source−drain current, I_d.

The transmission function is a measure of the strength of electron transmission through the various allowed channels, which in the present case are the participating one-electron molecular levels coupled to the metallic reservoirs (emitter/source and collector/drain). It is assumed here that the molecule is in contact with metals at two ends, referred to as the left and right electrodes.

$T(E,E_g)$ is the electron transmission function at a gate potential of V_g, which was obtained from the Green's function approach.[48,50]

$$T(E, E_g) = Tr[\Gamma_L(E, E_g)G(E, E_g)\Gamma_R(E, E_g)G^+(E, E_g)] \quad (4)$$

$$G(E, E_g) = [E \times I - H_{NT}(E, E_g) - \sum_L (E, E_g) - \sum_R (E, E_g)]^{-1} \quad (5)$$

where $H_{NT}(E,E_g)$ is the orthogonalized nonequilibrium Kohn−Sham (KS) Hamiltonian matrix of the active region of the device in the presence of the gate field obtained by a appropriate partitioning of $H^T(E,E_g)$[44] in eq 6, E is the injection energy of the tunneling electron, I is the identity matrix, and $\Gamma_{L(R)}(E,E_g)$ is twice the imaginary part of the self-energy matrices $\sum_{L(R)}^{V_g}$[50,51]

$$\sum_{L(R)}^{V_g} = C_{L(R)}^{+} G_{L(R)}^{V_g} C_{L(R)}$$

where $C_{L(R)}$ is the coupling matrix of the molecule and the left (right) metallic electrode. The total Hamiltonian of the system in the presence of the external electric fields due to V_g is represented as

$$H^T[E, E_g] = H^0 + H' + H'' \quad (6)$$

where H^0 is the Hamiltonian in the absence of external perturbations and H' and H'' represent perturbations due to applied gate field and the geometric perturbation applied at the gate arm, respectively. Essentially, $H' = -\vec{\varepsilon}_g \times \sum_i r_i$, where $\vec{\varepsilon}_g$ is the applied gate field and r_i is the coordinate of the ith electron, whereas H'' incorporates the change in the electronic structure properties due the geometric perturbations at the gate arm.

To observe the effect of voltage gating, the geometrical configuration of the molecular complex obtained at the zero field was used for all of the calculations assuming that the external electric field employed does not significantly modify the geometry of the architecture. The change in the total charge of the molecule is found to be negligible in the range of gate field considered because the molecular electrochemical potential remains confined in an energy range where the molecule has a very low density of states (DOS). The effect of the capacitance due to the charge redistribution under a nonzero gate field is taken into account via a self-consistent calculation. The Fock matrix F and overlap matrix S (corresponding to a nonorthogonal set of wave functions) from the Kohn−Sham solution of the extended molecule electronic structure calculation for each gate potential were used for electron transport calculations via eqs 1−4. To calculate the "conformational gating", the IC_2 in Figure 1 was further rotated by 30° and the I_d−V_{ds} were calculated according to the procedure described above.

3. RESULTS AND DISCUSSION

We consider the conformational changes in the device system in terms of the relative orientation of the phenyl rings in the "gate" arm, for example, rotation of IC_2 with regard to IC_1 by 30°. Specifically, the configurations considered are: (A) "O": the ground state configuration ("O") where IC_2 is out of plane by ∼ −30° (anticlockwise) with regard to IC_1.; (B) "A": IC_2 is given an anticlockwise rotation by 30° relative to the ground-state configuration, "O" (i.e., IC_2 is −60° out of plane with regard to IC_1); and (C) "B": IC_2 is given a clockwise rotation by 30° relative to the ground-state configuration, "O", making IC_2 and IC_1 almost planar in the architecture.

Figure 2 shows the effect of conformational change on the total energy of the system, showing that the anticlockwise rotation of IC_2 reduces the stability of the system slightly more than that of the clockwise rotation (energy barrier between state "A" and "O" is 0.18 eV and that of "O" and "B" is 0.13 eV).

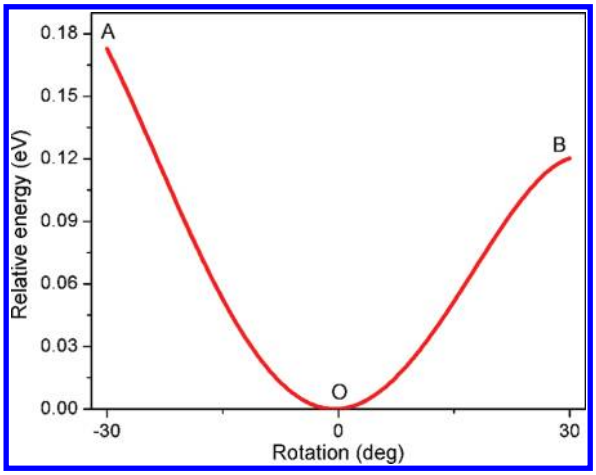

Figure 2. Effects of conformational changes at the gate arm of the molecules on its total energy of the system. The zero of energy is aligned to the ground-state energy of the system. "O" corresponds to the ground-state configuration and "A" and "B" represent the cases when IC_2 is rotated with regard to IC1 by 30°, anticlockwise and clockwise, respectively.

dx.doi.org/10.1021/jp208983d | J. Phys. Chem. C 2012, 116, 4840−4847

In the architecture described above (Figure 1), the effect of an applied field between the S and D ends acts as a perturbation to polarize the charge distribution and mix one-electron energy levels of the system. The additional perturbation along the G arm likely induces additional change in the spatial distribution of the electron charge density and therefore the one-electron energy levels of the system. Specifically, we consider:

(i) Conformational change in the gate molecule via rotation of IC_2 with regard to IC_1 (Figure 1)
(ii) Perturbation due to the electric field parallel to the gate arm, which is symmetric with respect to source and drain but asymmetric in the gate direction

First, we shall discuss the effects of these perturbations individually and then the combined effects of (i) and (ii).

3.A. Conformational Gating. In Figure 3, we show the effect of conformational changes at the gate arm of the molecule on its I_d–V_{ds} characteristics. When no gate voltage is applied, the three-terminal device should ideally behave like a two-terminal device. It may be seen from Figure 3 that the response of the device to the applied bias voltage is insignificant for configurations "O" and "B" even when the bias is high (V_{ds} = 2 V). The current rises steeply for the configuration "A" (i.e., IC_2 is out-of-plane relative to IC_1 by ~60°) with V_{ds} >1.6 V.

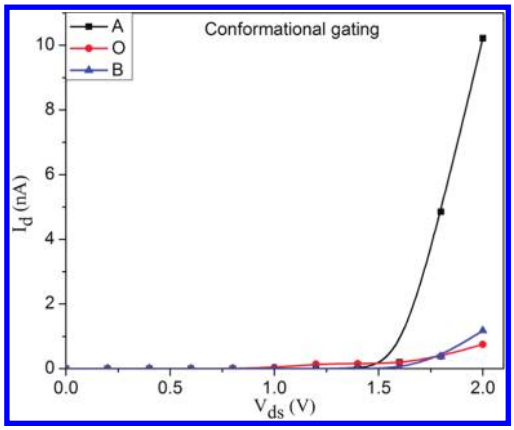

Figure 3. Effect of the conformational gating at the gate arm of the molecule on its I_d–V_{ds} curves. The "O" corresponds to the ground state and "A" and "B" correspond to 30° anticlockwise and clockwise rotation of IC_2 relative to the ground-state configuration of the device, respectively.

To understand the calculated I_d–V_{ds} characteristics, we examined the transmission functions, shown in Figure 4a, for all configurations. Considering Figure 4a, we clearly note a direct correlation between the magnitude of the transmission function and the tunneling current in the device system. For example, the transmission function associated with configuration "A" is much higher than that of the other two configurations, leading to a current an order of magnitude larger compared with those for other configurations. It is, therefore, evident that the conformational change in the unbiased branch of the molecule enhances the electron tunneling probability in the biased arms (conduction channel) in the present architecture. It is interesting to note that similar chemical gating effect, that is, conformational change in a branched arm of biological macromolecules, lead to significant changes in charge transfer across other ends of the molecule.[26−28] The same phenomenon also plays a key role in the modulation of chemical-gated ion-channel current, where conformational changes in transmembrane proteins opens or closes the ion-channel pores.[31]

To understand further the origin of the higher current in "A", we examined the effect of conformational gating on the MO energy levels of the complex architecture, shown in (Figure 5a). We notice that the conformational gating changes neither the highest occupied (HO)−lowest unoccupied (LU) MO gap of the system nor the dipole moment associated with "A" and "B" significantly from that of the ground state ("O"). However, a considerable rearrangement of the molecular energy levels takes place in the MO energy levels in the regime further down (HOMO-4 and below) (Figure 5a).

Figure 6a shows the nature of HOMO's in all the three cases, "O", "A", and "B", where it appears that the conformational gating affects the current via localization/delocalization of the electronic wave function in the conduction channel. For example, the wave function is relatively more localized toward the conduction channel for configuration "A", resulting in a higher transmission function as compared with that of "O" and "B". In other words, the nonplanar orientation of the π-electron moieties at the gate arm lifts the carriers up to the S-D channel from the G arm, leading to a high-conducting (ON) state for the system. Our results can be correlated with the role of conformational gating in the photosynthetic reaction center[30] and enzyme specificity where the conformational gating in the enzyme simply turns the active site to the inert toward the substrate and vice versa[32] via charge transfer mechanism. The current modulation (I_{ON}/I_{OFF}) by pure conformational gating (V_g = 0) is found to be ~14 at V_{ds} = 2 V (Figure 3).

3.B. Voltage Gating. For the voltage gating, the I_d–V_{ds} characteristics were found to be independent of gate field in the

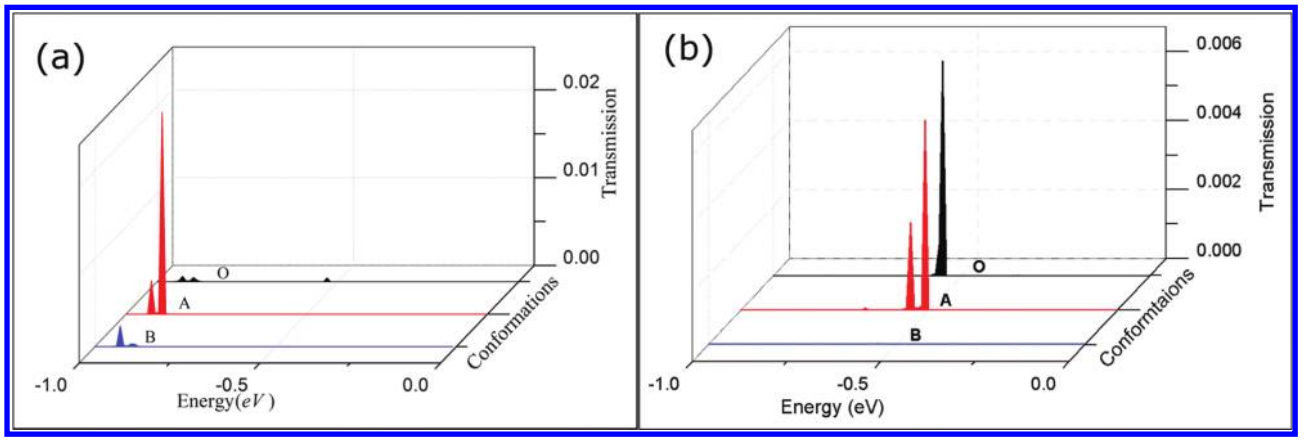

Figure 4. Effect of the conformational gating at the gate arm on the transmission functions responsible for the I_d–V_{ds} curves for (a) V_g = 0 and (b) V_g = 3 V.

dx.doi.org/10.1021/jp208983d | J. Phys. Chem. C 2012, 116, 4840−4847

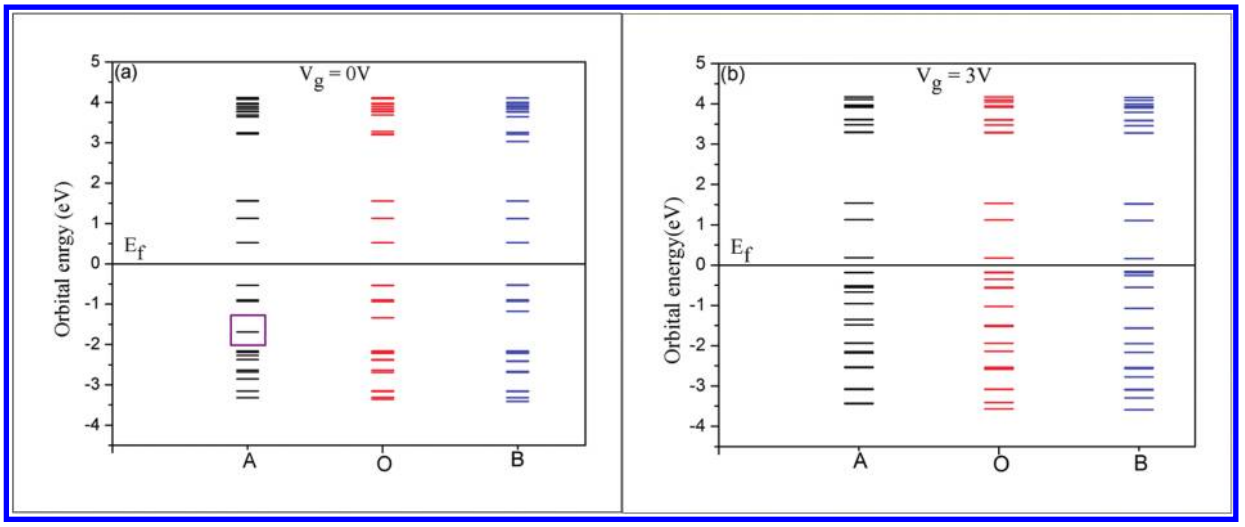

Figure 5. Evolution of molecular spectra of the extended molecule under (a) conformational gating and (b) both the conformational and voltage gating. Zero of the energy represents the Fermi energy of the system. A square indicates the significant rearrangement.

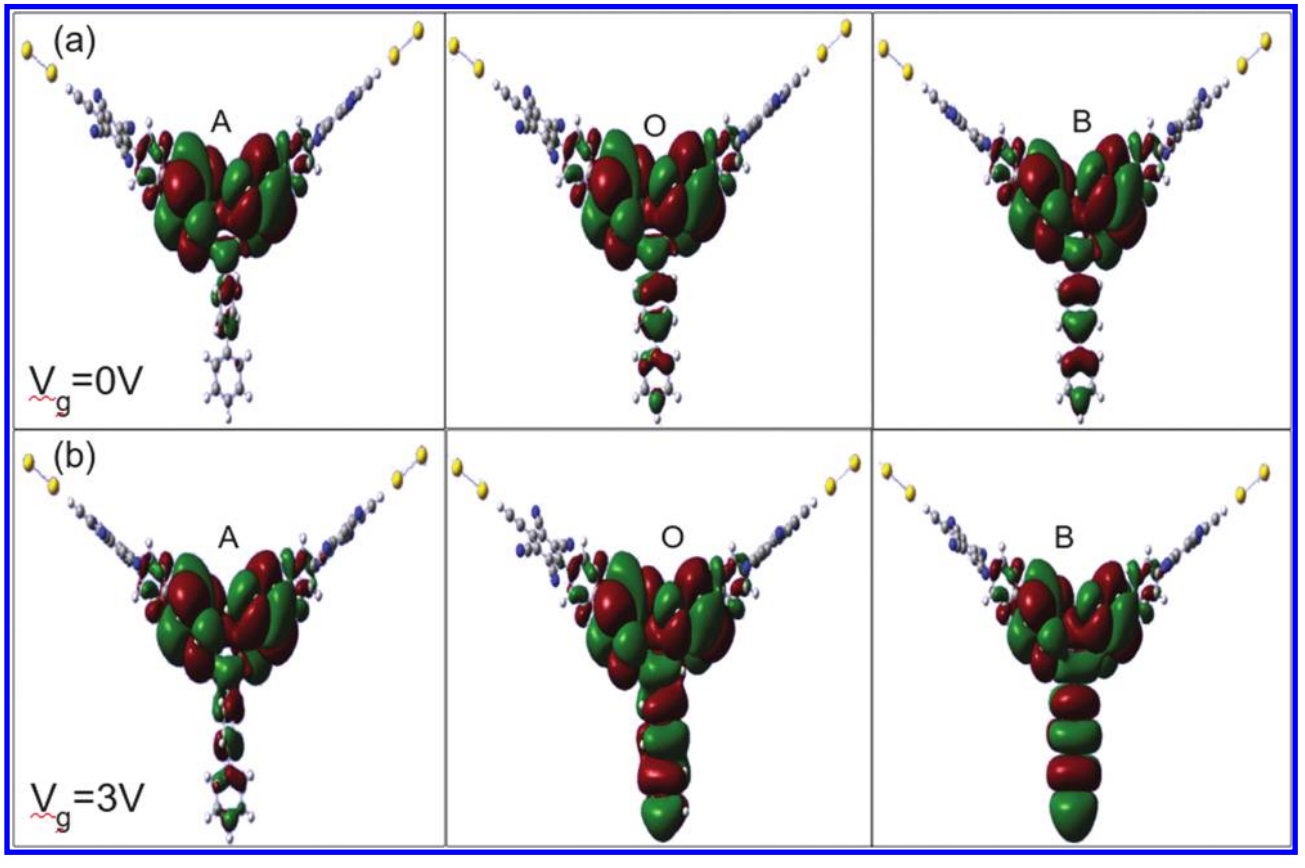

Figure 6. Evolution of HOMO for (a) conformational gating (i.e., "A", "O", and "B" configurations) and (b) both conformational and voltage gating. An isovalue of 0.002 e/bohr^3 (1/10th of the default) is used.

low bias field regime, that is, V_{ds} < 1 V. However, with increase in V_{ds}, I_d increases dramatically (Figure 7) due to the resonant tunneling, as previously discussed.[12,32] It has been previously noted that the intrinsic dipole moment and the induced polarization of the molecule due to the applied external perturbation play an important role on quantum transport in molecular systems.[33] Therefore, it is useful to examine the relationship of dipole moment, polarization, and energy-level mixing with the switching behavior noted here. Although the system has a zero dipole moment along the S-D arm, the polarity along the G arm produces a permanent dipole moment along the z direction, ensuring a strong electrostatic coupling between the gate arm and rest of the molecular architecture. Moreover, the dipole moment varies significantly and almost linearly with the external electric field. The positive field enhances the dipole moment and lowers the energy of the system. From the examination of the evolution of MO energy, He et al. explained that the gap between the MOs representing the donor (D) group and the acceptor (A) group narrows with a positive field (enhancement mode), and thus the current

dx.doi.org/10.1021/jp208983d | J. Phys. Chem. C 2012, 116, 4840–4847

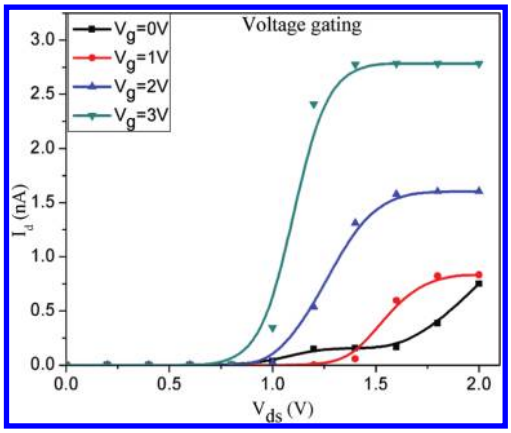

Figure 7. I_d–V_{ds} curves for the ground state of the device under various applied gate voltages.

increases significantly.[12] The current modulation reaches its maximum (I_{ON}/I_{OFF} = 160) when V_g = 3V at $V_{ds} \approx$ 1.4 V.

3.C. Conformational and Voltage Gating. When we consider the combined effects of the conformational changes and the gate field, the architecture shows a peculiar behavior in its I_d–V_{ds} characteristics. Application of the gate field in the conformational-gated "ON" state reduces the magnitude of current. For V_g = 1 V, the response of the device in configuration "B" to the bias voltage, V_{ds} > 1, dominates over the other configurations. The configurations "A" and "O" show a higher response current for V_g = 2 and 3 V at the lower bias voltage (V_{ds} = ~0.5 V) (Figure 8a–c). The current for "O", however, seems to increase steadily with increase in V_g (Figure 8a–c). It is clear that the effect of voltage gating in this three-terminal architecture critically depends on the geometry and shows a peculiar behavior when the system is away from the equilibrium geometry.

To summarize the combined effects, we looked into the so-called transfer curve (I_d vs V_g) for V_{ds} = 2 V in Figure 9. Here I_d for "O" increases steadily with V_g, as can be expected in the case of "voltage gating only" (Figure 7). For configurations "A" and "B", I_d shows diminishing oscillatory behavior with increasing V_g. It may also be noted that the magnitude of I_d oscillates in the cases of "A" and "B" with a phase factor of $\pi/2$. Note that the conformational changes given to IC_2 in "A" and "B" are opposite in nature, that is, anticlockwise and clockwise rotations, respectively. As the voltage gating is turned on, the magnitude of transmission function (Figure 4b) reduces significantly and thus explains the lower current for $V_g \neq 0$.

Despite the reduction in the HOMO–LUMO gap (Figure 5b) due the applied V_g, the magnitude of I_d decreases for a nonzero value of V_g. It may be due to the fact that V_g shifts MOs relative to the case of V_g = 0, affecting the rearrangement found in Figure 5a. For example, the wave function is more localized in the conduction channel when V_g = 0 (Figure 6a) for "A" relative to that when V_g = 3 V, shown in Figure 6b. Obviously, higher degree of localization of the electronic wave

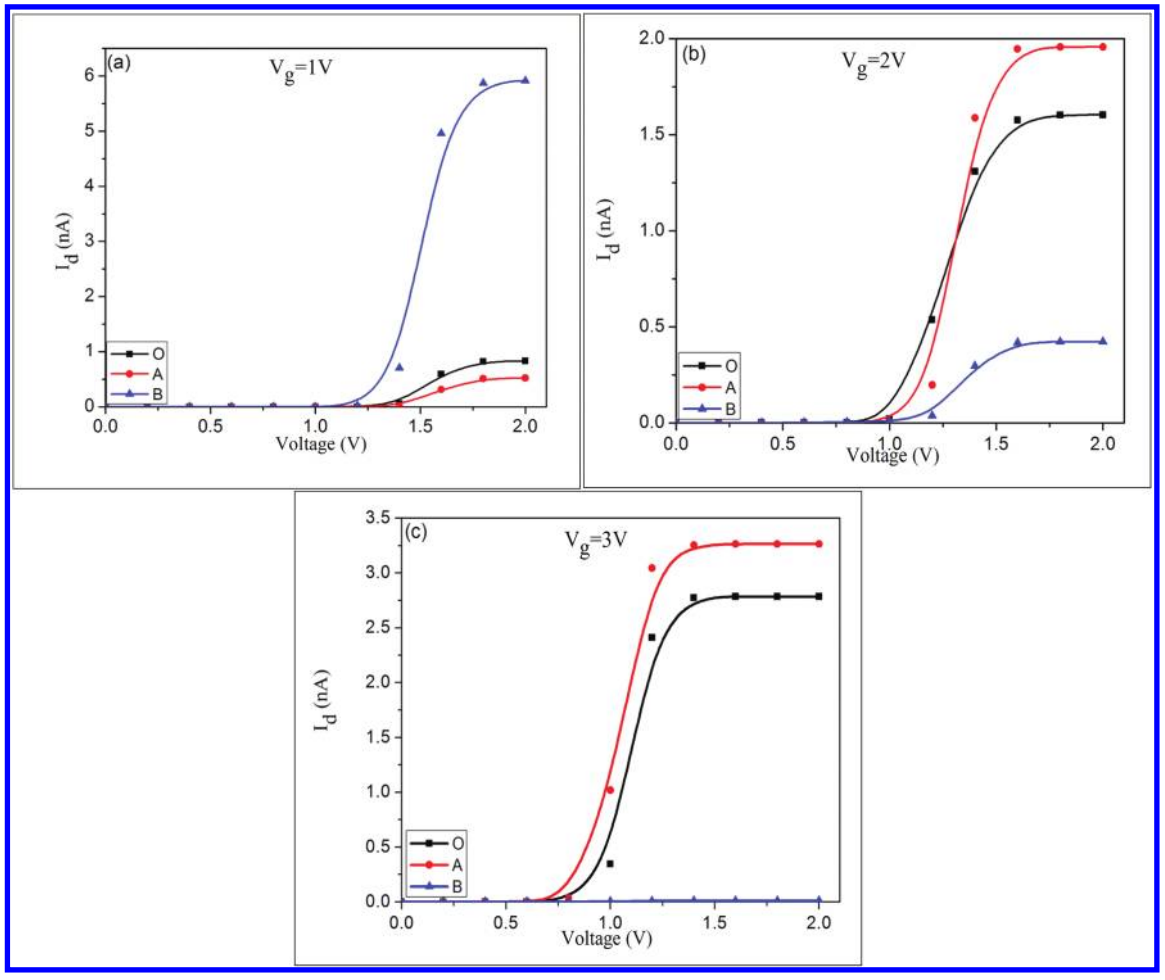

Figure 8. Effects of conformational and voltage gating; I_d–V_{ds} curves for all three conformations at: V_g = (a) 1, (b) 2, and (c) 3 V.

dx.doi.org/10.1021/jp208983d | J. Phys. Chem. C 2012, 116, 4840–4847

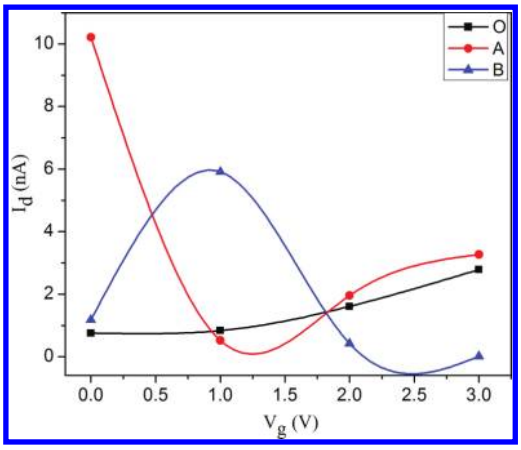

Figure 9. Transfer curve representing variation of I_d as a function of applied V_g at V_{ds} =2 V. The ground state of the device is "O". The current corresponding to the configuration "A" and "B" varies with the applied V_g with a phase factor of Π/2.

function along the conduction channel at V_g =3 V found in configuration "A" (Figure 6b) explains the higher transmission (Figure 4b) and therefore higher current in Figure 9.

The maximum current modulations with respect to the ground-state modulation [I_{ON}/I_{OFF}] are 7.1, 1.2, and 1.2 for V_g = 1, 2, and 3 V, respectively, in the presence of conformational and voltage gating. Note that the I_{ON}/I_{OFF} under the effect of exclusive conventional and conformational gating was found to be 160[12] and 14. Therefore, we may conclude that the current modulation reaches its maximum value when either conventional or conformational gating is applied and diminishes under their conjugal effects.

Although our objective in this study is to look into the possibility to control the current in a molecular transistor by conformational change instead of the conventional gating, it is worth mentioning that it is possible to rotate IC_2 relative to the rest of the gate-arm architecture experimentally. We are aware of the potential difficulties to achieve the above-mentioned conformational change via induced electric field effect,[52,53] which would possibly interfere with the gate field, and it would be difficult to distinguish their effects separately. In recent experiments, however, photoinduced conformational changes[54] and thereby realization of electronic switches[55,56] in metal−molecule−metal junctions have been a viable practice. Because inclusion of a third electrode (for voltage gating) is likely to change the molecular geometry that the performance of the transistor critically depends on (Figure 9), it might be more desirable to implement the photon-assisted conformational gating via UV-irradiation[56] in real experiments.

4. SUMMARY

In summary, a nonplanar orientation of IC_2 at the gate arm leads to a highly conductive "ON" state of three-terminal molecular architecture under biased conditions due to the charge transfer from the gate arm to the conduction arm (channel) of the molecule. This is similar to the conformational gating effect in biological processes such as photosynthetic reaction centers and enzyme specificity. The current modulation reaches its maximum only under the exclusive effect of voltage or conformational gating and decreases when both of them are present. In the presence of the voltage gating, the tunneling current corresponding to conformational gating in two different directions appears to exhibit oscillatory nature with a phase factor of $\pi/2$.

■ ASSOCIATED CONTENT

Supporting Information

Comparative study on the validity of the assumptions and accuracy employed in this study. This material is available free of charge via the Internet at http://pubs.acs.org.

■ AUTHOR INFORMATION

Corresponding Author

*(R.P.) E-mail: pandey@mtu.edu; Tel: 906.487.2086. (S.P.K.) E-mail: Shashi.p.karna.civ@mail.mil; Tel: 410.306.0723.

Notes

The authors declare no competing financial interest.

■ ACKNOWLEDGMENTS

The helpful discussions with Haiying He, Ranjit Pati, and Wil Slough are acknowledged. The work at Michigan Technological University was performed under support by Army Research Office through contract number W911NF-09-1-0221.

■ REFERENCES

(1) Kagan, C. R.; Afzali, A.; Martel, R.; Gignac, L. M.; Solomon, P. M.; Schrott, A. G.; Ek, B. *Nano Lett.* **2003**, *3*, 119−124.
(2) Keane, Z. K.; Ciszek, J. W.; Tour, J. M.; Natelson, D. *Nano Lett.* **2006**, *6*, 1518−1521.
(3) Lee, J. O.; Lientschnig, G.; Wiertz, F.; Struijk, M.; Janssen, R. A. J.; Egberink, R.; Reinhoudt, D. N.; Hadley, P.; Dekker, C. *Nano Lett.* **2003**, *3*, 113−117.
(4) Song, H.; Kim, Y.; Jang, Y. H.; Jeong, H.; Reed, M. A.; Lee, T. *Nature* **2009**, *462*, 1039−1043.
(5) Xu, B. Q.; Xiao, X. Y.; Yang, X. M.; Zang, L.; Tao, N. J. *J. Am. Chem. Soc.* **2005**, *127*, 2386−2387.
(6) Yu, L. H.; Keane, Z. K.; Ciszek, J. W.; Cheng, L.; Stewart, M. P.; Tour, J. M.; Natelson, D. *Phys. Rev. Lett.* **2004**, *93*, 266802−266805.
(7) Yu, L. H.; Natelson, D. *Nano Lett.* **2004**, *4*, 79−83.
(8) Bratkovsky, A. M.; Kornilovitch, P. E. *Phys. Rev. B: Condens. Matter Mater. Phys.* **2003**, *67*, 115307−115313.
(9) Choi, Y. C.; Kim, W. Y.; Park, K. S.; Tarakeshwar, P.; Kim, K. S.; Kim, T. S.; Lee, J. Y. *J. Chem. Phys.* **2005**, *122*, 094706−094711.
(10) Di Ventra, M.; Pantelides, S. T.; Lang, N. D. *Appl. Phys. Lett.* **2000**, *76*, 3448−3450.
(11) Ghosh, A. W.; Rakshit, T.; Datta, S. *Nano Lett.* **2004**, *4*, 565−568.
(12) He, H.; Pandey, R.; Karna, S. P. *Nanotechnology* **2008**, *19*, 505203−505208.
(13) Hod, O.; Baer, R.; Rabani, E. *J. Am. Chem. Soc.* **2005**, *127*, 1648−1649.
(14) Ke, S. H.; Baranger, H. U.; Yang, W. T. *Phys. Rev. B* **2005**, *71*, 113401−113404.
(15) Perrine, T. M.; Dunietz, B. D. *Phys. Rev. B* **2007**, *75*, 195319−195324.
(16) Perrine, T. M.; Smith, R. G.; Marsh, C.; Dunietz, B. D. *J. Chem. Phys.* **2008**, *128*, 154706−154712.
(17) Son, Y. W.; Ihm, J.; Cohen, M. L.; Louie, S. G.; Hyoung Joon, C. *Phys. Rev. Lett.* **2005**, *95*, 216602−216605.
(18) Yang, Z. Q.; Lang, N. D.; Di Ventra, M. *Appl. Phys. Lett.* **2003**, *82*, 1938−1940.
(19) Andrews, D. Q.; Solomon, G. C.; Van Duyne, R. P.; Ratner, M. A. *J. Am. Chem. Soc.* **2008**, *130*, 17309−17319.
(20) Galperin, M.; Ratner, M. A.; Nitzan, A.; Troisi, A. *Science* **2008**, *319*, 1056−1060.
(21) Joachim, C.; Gimzewski, J. K.; Aviram, A. *Nature* **2000**, *408*, 541−548.
(22) Kubatkin, S.; Danilov, A.; Hjort, M.; Cornil, J.; Bredas, J. L.; Stuhr-Hansen, N.; Hedegard, P.; Bjornholm, T. *Nature* **2003**, *425*, 698−701.

(23) Liang, W. J.; Shores, M. P.; Bockrath, M.; Long, J. R.; Park, H. *Nature* **2002**, *417*, 725−729.
(24) Park, J.; Pasupathy, A. N.; Goldsmith, J. I.; Chang, C.; Yaish, Y.; Petta, J. R.; Rinkoski, M.; Sethna, J. P.; Abruna, H. D.; McEuen, P. L.; Ralph, D. C. *Nature* **2002**, *417*, 722−725.
(25) Reed, M. A.; Zhou, C.; Muller, C. J.; Burgin, T. P.; Tour, J. M. *Science* **1997**, *278*, 252−254.
(26) Graige, M. S.; Feher, G.; Okamura, M. Y. *Proc. Natl. Acad. Sci. U.S.A.* **1998**, *95*, 11679−11684.
(27) Walden, S. E.; Wheeler, R. A. *J. Phys. Chem. B* **2002**, *106*, 3001−3006.
(28) Xu, Q.; Gunner, M. R. *Biochemistry* **2002**, *41*, 2694−2701.
(29) Balabin, I. A.; Onuchic, J. N. *Science* **2000**, *290*, 114−117.
(30) Rabenstein, B.; Ullmann, G. M.; Knapp, E. W. *Biochemistry* **2000**, *39*, 10487−10496.
(31) Baker, K. A.; Tzitzilonis, C.; Kwiatkowski, W.; Choe, S.; Riek, R. *Nature Structural & Molecular Biology* **2007**, *14*, 1089−1095.
(32) Zhou, H. X.; Wlodek, S. T.; McCammon, J. A. *Proc. Natl. Acad. Sci. U.S.A.* **1998**, *95*, 9280−9283.
(33) Davis, W. B.; Ratner, M. A.; Wasielewski, M. R. *J. Am. Chem. Soc.* **2001**, *123*, 7877−7886.
(34) Pati, R.; Karna, S. P. *Phys. Rev. B* **2004**, *69*, 155419−155423.
(35) Venkataraman, L.; Klare, J. E.; Nuckolls, C.; Hybertsen, M. S.; Steigerwald, M. L. *Nature* **2006**, *442*, 904−907.
(36) Lang, N. D.; Solomon, P. M. *Nano Lett.* **2005**, *5*, 921−924.
(37) Lang, N. D.; Kagan, C. R. *Nano Lett.* **2006**, *6*, 2955−2958.
(38) Yaliraki, S. N.; Kemp, M.; Ratner, M. A. *J. Am. Chem. Soc.* **1999**, *121*, 3428−3434.
(39) Lamoen, D.; Ballone, P.; Parrinello, M. *Phys. Rev. B* **1996**, *54*, 5097−5105.
(40) Becke, A. D. *J. Chem. Phys.* **1993**, *98*, 5648−5652.
(41) Lee, C. T.; Yang, W. T.; Parr, R. G. *Phys. Rev. B* **1988**, *37*, 785−789.
(42) Frisch, M. J.; Trucks, G. W.; Schlegel, H. B.; Scuseria, G. E.; Robb, M. A.; Cheeseman, J. R.; Montgomery, J. A., Jr.; Vreven, T.; Kudin, K. N.; Burant, J. C. et al. *Gaussian 03*, 03 ed.; Gaussian, Inc: Pittsburgh, PA, 2003.
(43) He, H. Y.; Pandey, R.; Mallick, G.; Karna, S. P. *J. Phys. Chem. C* **2009**, *113*, 1575−1579.
(44) Pati, R.; McClain, M.; Bandyopadhyay, A. *Phys. Rev. Lett.* **2008**, *100*, 246801−246804.
(45) Thygesen, K. S.; Rubio, A. *Phys. Rev. B* **2008**, *77*, 115333−115354.
(46) Barraza-Lopez, S.; Park, K.; Garcia-Suarez, V.; Ferrer, J. *Phys. Rev. Lett.* **2009**, *102*, 246801−246804.
(47) Buttiker, M. *Phys. Rev. Lett.* **1986**, *57*, 1761−1764.
(48) Datta, S. *Electronic Transport Properties in Mesoscopic Systems*; Cambridge University Press: Cambridge, U.K., 1995.
(49) Landauer, R. *J. Phys.: Condens. Matter* **1989**, *1*, 8099−8110.
(50) Tian, W. D.; Datta, S.; Hong, S. H.; Reifenberger, R.; Henderson, J. I.; Kubiak, C. P. *J. Chem. Phys.* **1998**, *109*, 2874−2882.
(51) He, H. Y.; Pandey, R.; Karna, S. P. *Chem. Phys. Lett.* **2007**, *439*, 110−114.
(52) Lastapis, M.; Martin, M.; Riedel, D.; Hellner, L.; Comtet, G.; Dujardin, G. *Science* **2005**, *308*, 1000−1003.
(53) Moresco, F.; Meyer, G.; Rieder, K. H.; Tang, H.; Gourdon, A.; Joachim, C. *Phys. Rev. Lett.* **2001**, *86*, 672−675.
(54) Chang, C. W.; Lu, Y. C.; Wang, T. T.; Diau, E. W. G. *J. Am. Chem. Soc.* **2004**, *126*, 10109−10118.
(55) Choi, B. Y.; Kahng, S. J.; Kim, S.; Kim, H.; Kim, H. W.; Song, Y. J.; Ihm, J.; Kuk, Y. *Phys. Rev. Lett.* **2006**, *96*, 156106−156109.
(56) Mativetsky, J. M.; Pace, G.; Elbing, M.; Rampi, M. A.; Mayor, M.; Samori, P. *J. Am. Chem. Soc.* **2008**, *130*, 9192−9193.